

干涉偏差对四束圆偏振光干涉的影响

吴晓

浙江外国语学院科学技术学院, 浙江 杭州 310021

摘要 通过理论计算和 MATLAB 模拟讨论四束右旋圆偏振干涉光干涉后的光强度分布。当四束干涉光对称分布时,可得均匀的二维周期性强度分布。理论研究发现,干涉强度的最大值出现在 3 条直线斜率分别为 $S_1 = +1$, $S_2 = \infty$, $S_3 = -1$ 的交点处,且在 x 和 y 方向存在一定的周期 $d_x = d_y = \lambda / \sin \theta$ 。入射角的不同只改变周期的大小,不改变干涉强度分布的图样。研究发现,当其中一束干涉光发生偏差 (θ_1, α_1) 时,决定干涉强度的其中 2 条直线的斜率 $S_l (l=1,2)$ 以及 x 和 y 方向的周期 $d_{xl}, d_{yl} (l=1,2,3)$ 均受影响。

关键词 激光光学; 干涉; 干涉偏差; 斜率; 强度调制

中图分类号 O436.1

文献标识码 A

doi: 10.3788/LOP55.061405

Influence of Interference Deviation on Four-Beam Interference with Circular Polarization

Wu Xiao

School of Science and Technology, Zhejiang International Studies University, Hangzhou, Zhejiang 310021, China

Abstract The interference intensity distribution of four-beam interference with right-hand circular polarization is theoretically studied and simulated with MATLAB. The impact of incident angle on the intensity distribution of interference is studied. The results show that there is a uniform two-dimensional periodic intensity distribution when four beams show symmetrical distribution. The peak intensity appears at the intersection of three lines with the slopes of $S_1 = +1$, $S_2 = \infty$, $S_3 = -1$, respectively. And there are certain periods $d_x = d_y = \lambda / \sin \theta$ in the x and y directions. When incidence angle θ changes, the period of the pattern changes accordingly but not the symmetry of pattern. However, when the incident angle or azimuthal angle (θ_1, α_1) changes, both the slopes $S_l (l=1,2)$ and periods $d_{xl}, d_{yl} (l=1,2,3)$ change.

Key words laser optics; interference; interference deviation; slope; intensity modulation

OCIS codes 140.3430; 260.5430

1 引言

激光干涉技术由于其制造过程用时短且能实现大面积均匀分布的周期性结构而被广泛地应用于制造光子晶体、光波导、滤光片等电子器件^[1-15]。通过设置发生干涉光束的数目和曝光次数,可以得到多维的任意周期性结构。其中,四光束干涉技术仅利用单次曝光就能得到二维周期性结构,并已逐渐用于制造微纳级的多维周期性结构^[16-19]。近年来,文献^[20-24]已研究干涉强度分布对入射光束偏振态的依赖性,发现了干涉光束的入射角和光强的偏差会影响干涉图形。为了更好地用四光束干涉

技术实现微纳周期结构,有必要通过理论研究来认识四光束干涉原理,进一步分析干涉偏差对四光束干涉的影响。

本文对四束均为右旋圆偏振(RC)的干涉光的干涉现象进行理论计算和 MATLAB 模拟研究,并从入射角和方位角设置方面,详细讨论了当干涉光束对称分布和当其中一束干涉光存在偏差时对干涉强度分布产生的影响。

2 四束右旋圆偏振光干涉理论

图 1(a)为干涉光束在直角坐标系中的位置表示,图 1(b)为四束右旋圆偏振光干涉示意图,四束

收稿日期: 2017-10-12; 收到修改稿日期: 2017-12-03

作者简介: 吴晓(1985—),女,博士,讲师,主要从事光子晶体制造技术等方面的研究。E-mail: xwu@zisu.edu.cn

干涉光(B1,B2,B3,B4)的入射角 θ (与 z 轴夹角)和方位角 α (入射光在 xy 平面投影与 x 轴正方向的夹角)分别表示为 $\theta_1, \theta_2, \theta_3, \theta_4$ 与 $\alpha_1, \alpha_2, \alpha_3, \alpha_4$ 。假设四束干涉光均为平面波,初始相位为0且电场幅度均为 A ,则它们的电场 $\mathbf{E}_1(\mathbf{r}, t), \mathbf{E}_2(\mathbf{r}, t), \mathbf{E}_3(\mathbf{r}, t), \mathbf{E}_4(\mathbf{r}, t)$ 可分别表示为

$$\begin{cases} \mathbf{E}_1(\mathbf{r}, t) = \text{Re}\{A \exp[i(\mathbf{k}_1 \cdot \mathbf{r} - \omega t)]\mathbf{e}_1\} \\ \mathbf{E}_2(\mathbf{r}, t) = \text{Re}\{A \exp[i(\mathbf{k}_2 \cdot \mathbf{r} - \omega t)]\mathbf{e}_2\} \\ \mathbf{E}_3(\mathbf{r}, t) = \text{Re}\{A \exp[i(\mathbf{k}_3 \cdot \mathbf{r} - \omega t)]\mathbf{e}_3\} \\ \mathbf{E}_4(\mathbf{r}, t) = \text{Re}\{A \exp[i(\mathbf{k}_4 \cdot \mathbf{r} - \omega t)]\mathbf{e}_4\} \end{cases}, \quad (1)$$

式中: \mathbf{k}_n ($n=1, 2, 3, 4$)和 \mathbf{e}_n ($n=1, 2, 3, 4$)分别为对

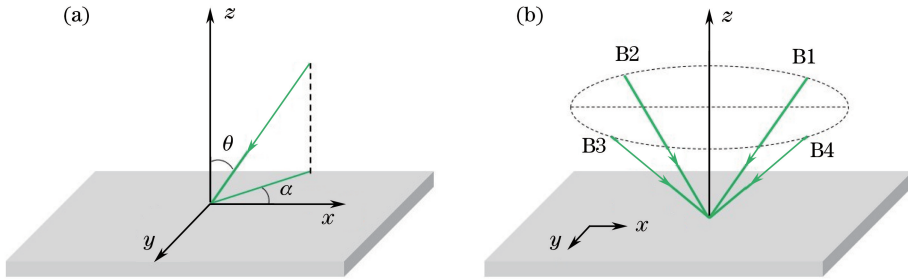


图1 (a)干涉光束在直角坐标系中的位置表示;(b)四束光(B1,B2,B3,B4)干涉的示意图

Fig. 1 (a) Interference beam in rectangular coordinate system; (b) diagram of four beams (B1, B2, B3, B4) interference

沿 z 轴传播的右旋圆偏振光的 Jones 矩阵和波矢可表示为 $\mathbf{J} = 1/\sqrt{2} (1 \ -i \ 0)^T$ 和 $\mathbf{k}_0 = (0 \ 0 \ k_0)^T$ ^[18]。根据旋转矩阵

$$\mathbf{R}_n(\theta_n, \alpha_n) = \begin{pmatrix} \cos \alpha_n \cos \theta_n & -\sin \alpha_n & \cos \alpha_n \sin \theta_n \\ \sin \alpha_n \cos \theta_n & \cos \alpha_n & \sin \alpha_n \sin \theta_n \\ -\sin \theta_n & 0 & \cos \theta_n \end{pmatrix}, \quad (4)$$

可得:干涉时,四束光的波矢和偏振态的单位矢量分别为

$$\begin{aligned} \mathbf{k}_n &= \mathbf{R}_n \mathbf{k}_0 = \begin{pmatrix} \cos \alpha_n \sin \theta_n \\ \sin \alpha_n \sin \theta_n \\ \cos \theta_n \end{pmatrix} \mathbf{k}_0, \\ \mathbf{e}_n &= \mathbf{R}_n \mathbf{J} = \frac{1}{\sqrt{2}} \begin{pmatrix} \cos \alpha_n \cos \theta_n + i \sin \alpha_n \\ \sin \alpha_n \cos \theta_n - i \cos \alpha_n \\ -\sin \theta_n \end{pmatrix}. \end{aligned} \quad (5)$$

当四束干涉光对称分布于 z 轴周围时,即 $\theta_1 = \theta_2 = \theta_3 = \theta_4 = \theta, \alpha_1 = 0^\circ, \alpha_2 = 90^\circ, \alpha_3 = 180^\circ, \alpha_4 = 270^\circ$,将(4)式和(5)式代入表示干涉强度的(3)式,可得

$$I_T \propto 4A^2 + \frac{A^2}{2} \{2\cos[k_0(x-y)\sin\theta]\sin^2\theta + 4\sin[k_0(x-y)\sin\theta]\cos\theta - 2\cos(2k_0x\sin\theta)\cos^2\theta + 2\cos[k_0(x+y)\sin\theta]\sin^2\theta + 4\sin[k_0(x+y)\sin\theta]\cos\theta + 2\}. \quad (6)$$

从(6)式可得,四束对称分布的干涉光干涉后其强度分布与 z 轴无关,且在 xy 平面内出现二维周期性结构分布,如图2(a)所示。同时,可得干涉强度的最大值出现在直线斜率为 $S_1 = +1, S_2 = \infty, S_3 = -1$ 的交点处($S_2 = \infty$ 即平行于 y 轴的直线),且沿 x 轴和 y 轴方向存在一定的周期: $d_{x1} = \lambda/\sin\theta, d_{x2} = \lambda/(2\sin\theta), d_y = \lambda/\sin\theta$ 。当同时改变四束干涉光的入射角时,干涉图像的二维周期性分布不会发生变化,只是沿着 x 轴和 y 轴方向

的周期发生了变化,如图2(b)和(c)所示。

3 干涉偏差分析

当入射光束中的一束干涉光发生偏差,即入射角和方位角分别为: $\theta_1 \neq \theta, \theta_2 = \theta_3 = \theta_4 = \theta; \alpha_1 \neq 0^\circ, \alpha_2 = 90^\circ, \alpha_3 = 180^\circ, \alpha_4 = 270^\circ$ 。当 $\theta_1 = \theta, \alpha_1 = 0^\circ$ 时,即四束圆偏振干涉光对称分布时,干涉强度满足(6)式,且沿 z 轴方向不出现强度调制现象,如图3(a1)~(a2)所示。将以上参数代入(4)式和(5)式,干涉后(3)式变为

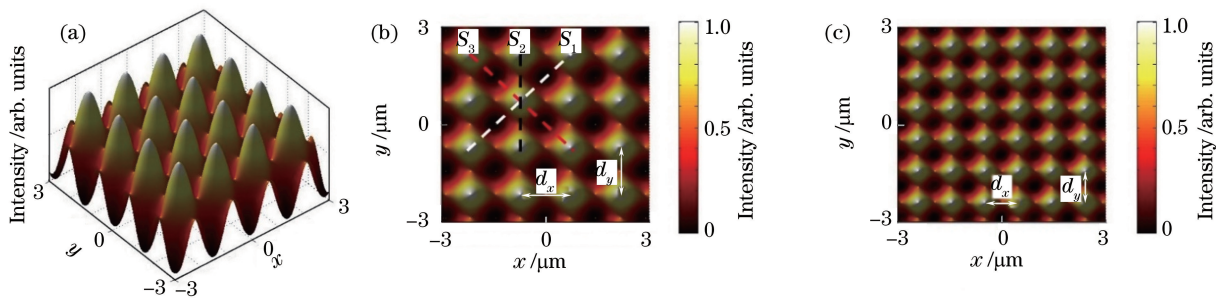


图2 利用 MATLAB 模拟得到四束对称分布的右旋圆偏振干涉光束干涉强度分布。(a)干涉强度分布的三维视图；(b)入射角为 $\theta=10^\circ$ 时干涉强度在 xy 平面内的分布；(c)入射角为 $\theta=15^\circ$ 时干涉强度在 xy 平面内的分布

Fig. 2 Interference intensity distributions of four symmetrical RC interference beams using MATLAB simulation.

(a) 3-dimensional view of intensity distribution; (b) intensity distribution in xy -plane with the incidence angle $\theta=10^\circ$; (c) intensity distribution in xy -plane with the incidence angle $\theta=15^\circ$

$$\begin{aligned}
 I_T \propto & 4A^2 + \frac{A^2}{2} \{ 2\cos\{k_0[x\sin\theta_1\cos\alpha_1 + y(\sin\theta_1\sin\alpha_1 - \sin\theta) + z(\cos\theta_1 - \cos\theta)]\}(\sin\alpha_1 + \\
 & \sin\theta_1\sin\theta + \sin\alpha_1\cos\theta\cos\theta_1) + 2\sin\{k_0[x\sin\theta_1\cos\alpha_1 + y(\sin\theta_1\sin\alpha_1 - \sin\theta) + \\
 & z(\cos\theta_1 - \cos\theta)]\}(\cos\alpha_1\cos\theta_1 + \cos\alpha_1\cos\theta) + \cos\{k_0[x(\sin\theta_1\cos\alpha_1 + \sin\theta) + y\sin\theta_1\sin\alpha_1 + \\
 & z(\cos\theta_1 - \cos\theta)]\}(-\cos\alpha_1 + \sin\theta_1\sin\theta - \cos\alpha_1\cos\theta\cos\theta_1) + \sin\{k_0[x(\sin\theta_1\cos\alpha_1 + \sin\theta) + \\
 & y\sin\theta_1\sin\alpha_1 + z(\cos\theta_1 - \cos\theta)]\}(\sin\alpha_1\cos\theta + \sin\alpha_1\cos\theta_1) + \\
 & 2\cos[k_0(x+y)\sin\theta]\sin^2\theta + 4\sin[k_0(x+y)\sin\theta]\cos\theta + 2 \}. \quad (7)
 \end{aligned}$$

由(7)式可知,入射角 θ_1 的偏差使干涉后强度在 z 轴方向出现调制现象,如图3(b1)~(b2)所示, z 轴方向的周期 $d_z = \lambda/|\cos\theta_1 - \cos\theta|$, θ_1 与 θ 相差越大,调制现象会越明显。而方位角的偏差未使干涉后强度在 z 轴方向出现调制现象,如图3(c1)~(c2)所示。对于垂直于 z 轴的某一个 xy 平面,强度图样同时受入射角和方位角的影响。出现强度最

大值的3条直线(l 代表直线数)中有2条直线的斜率会随着入射角 θ_1 的偏差发生变化,同时,沿着 x 轴和 y 轴方向的周期也发生变化,如表1所示,表中 S_l ($l=1,2,3$)表示干涉强度分布出现最大时的直线所对应的斜率; d_{xl}, d_{yl} ($l=1,2,3$)分别表示对应沿着 x 轴和 y 轴方向存在的周期。

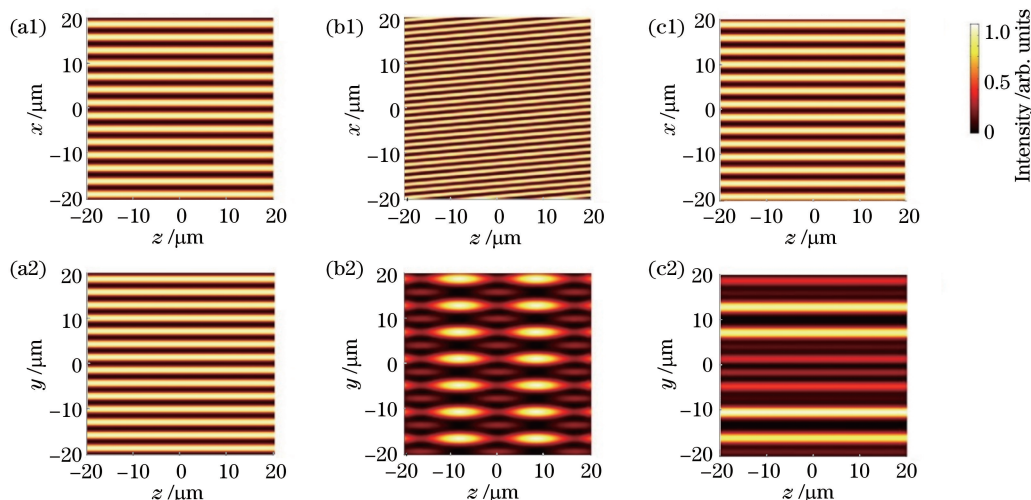


图3 四束干涉光沿 xz 轴和 yz 轴方向的干涉强度分布。(a1)、(a2)对称分布;(b1)、(b2)入射角发生偏差时;(c1)、(c2)方位角发生偏差时

Fig. 3 Interference intensity distributions along the xz -axis and yz -axis. (a1)(a2) Symmetrical distribution; (b1)(b2) under incidence deviation; (c1)(c2) under azimuth deviation

表 1 干涉强度分布出现最大值的直线所对应的斜率和干涉周期

Table 1 Slope of lines and interference periods where the maximum interference intensity appears

Parameter	$l=1$	$l=2$	$l=3$
S_l	$S_1 = -\frac{\sin \theta_1 \cos \alpha_1}{\sin \theta_1 \sin \alpha_1 - \sin \theta}$	$S_2 = -\frac{\sin \theta_1 \cos \alpha_1 + \sin \theta}{\sin \theta_1 \sin \alpha_1}$	$S_3 = -1$
d_{x1}	$d_{x1} = \frac{\lambda}{\sin \theta_1 \cos \alpha_1}$	$d_{x2} = \frac{\lambda}{\sin \theta_1 \cos \alpha_1 + \sin \theta}$	$d_{x3} = \frac{\lambda}{\sin \theta}$
d_{y1}	$d_{y1} = \frac{\lambda}{ \sin \theta_1 \sin \alpha_1 - \sin \theta }$	$d_{y2} = \frac{\lambda}{\sin \theta_1 \sin \alpha_1}$	$d_{y3} = \frac{\lambda}{\sin \theta}$
d_z		$d_z = \frac{\lambda}{ \cos \theta_1 - \cos \theta }$	

如表 2 所示,把造成偏差的原因分为:入射角 θ_1 偏差和方位角 α_1 偏差。可以得到:当入射角发生偏差时,其中一个斜率受到 θ_1 的影响 ($S_1 = \sin \theta_1 / \sin \theta$),所以当入射角偏差越大 (θ_1 与 θ 相差

越大)时,干涉强度调制现象越明显。方位角 α_1 的偏差不仅会影响斜率,而且也影响在 xy 平面内干涉强度分布的周期,这使得干涉强度分布图出现明显的强度调制。

表 2 当入射角或方位角发生偏差时,所对应的斜率和干涉周期

Table 2 Slope of lines and interference periods when there is a deviation in the incident angle or azimuth angle

Parameter	Deviation of incident angle	Deviation of azimuth angle
S_l	$S_1 = \frac{\sin \theta_1}{\sin \theta}, S_2 = \infty, S_3 = -1$	$S_1 = -\frac{\cos \alpha_1}{\sin \alpha_1 - 1}, S_2 = -\frac{\cos \alpha_1 + 1}{\sin \alpha_1}, S_3 = -1$
d_{x1}	$d_{x1} = \frac{\lambda}{\sin \theta_1}, d_{x2} = \frac{\lambda}{\sin \theta + \sin \theta_1}, d_{x3} = \frac{\lambda}{\sin \theta}$	$d_{x1} = \frac{\lambda}{\sin \theta \cos \alpha_1}, d_{x2} = \frac{\lambda}{\sin \theta (\cos \alpha_1 + 1)}, d_{x3} = \frac{\lambda}{\sin \theta}$
d_{y1}	$d_{y1} = \frac{\lambda}{\sin \theta}, d_{y2} = \infty, d_{y3} = \frac{\lambda}{\sin \theta}$	$d_{y1} = \frac{\lambda}{\sin \theta (1 - \sin \alpha_1)}, d_{y2} = \frac{\lambda}{\sin \alpha_1 \sin \theta}, d_{y3} = \frac{\lambda}{\sin \theta}$
d_z	$d_z = \frac{\lambda}{ \cos \theta_1 - \cos \theta }$	$d_z = \infty$

应用 MATLAB 程序,得到一束干涉光出现偏差 (θ_1, α_1) 时,在 xy 平面内的四光束干涉强度分布,如图 4 所示。与四束对称分布的圆偏振干涉光束干涉强度分布相比,只要四束干涉光中任意一束光的入射角或者方位角发生偏差,干涉图像就会出现调制。当入射角发生偏差时,如图 4(a) 所示,沿

x 轴方向出现多个周期,但是在 y 轴方向,其周期性仍然是 $d_{y1} = \lambda / \sin \theta$ 。因此,整个调制主要发生在水平方向上,干涉图像出现准周期性分布。若方位角发生偏差,在 x 轴和 y 轴方向上均出现多个周期性,这使得干涉后出现明显的强度调制现象,如图 4(b) 所示。

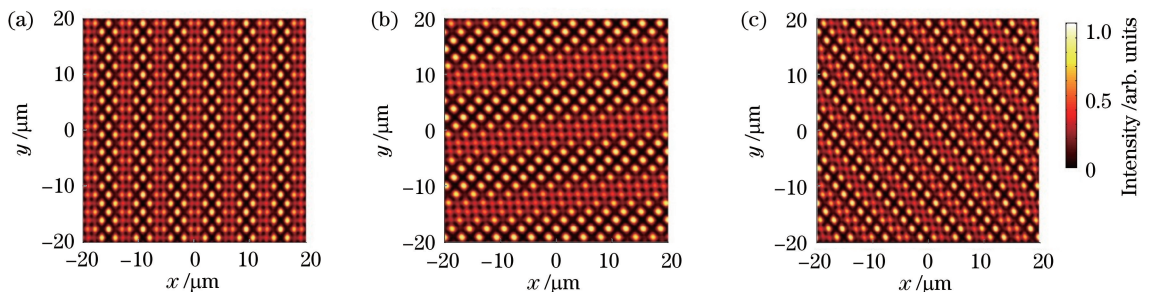


图 4 干涉强度分布图。(a)入射角发生偏差时;(b)方位角发生偏差时;(c)入射角和方位角都发生偏差时

Fig. 4 Interference intensity distributions. (a) Under azimuth deviation; (b) under azimuth deviation;

(c) under both incidence and azimuth deviations

4 结 论

综上所述,研究了四束右旋圆偏振光的干涉过

程,分析其中一束光的入射角和方位角发生偏差对干涉强度分布的影响。通过理论推导,得出对于四束对称分布的干涉光,干涉后得到均匀的二维周期

性强度分布,且沿着 x 轴和 y 轴方向的周期相同,均为 $\lambda/\sin\theta$ 。鉴于该特点,四光束干涉技术有时可以取代双光束两次干涉,用于制作二维周期性结构^[10]。通过理论计算发现,四光束干涉过程中,干涉依赖入射角和方位角。入射角或方位角偏差会影响斜率 S_i 以及沿 x, y, z 轴的周期,从而使得干涉后的强度分布出现调制现象,且出现的分布图为准周期性结构。同时,从干涉理论出发,发现当入射角发生偏差时,在 z 轴方向上出现强度调制,即 $d_z = \lambda/|\cos\theta_1 - \cos\theta|$;而方位角的偏差并未影响 z 轴方向强度分布。通过对四光束干涉的理论推导计算以及仿真模拟得出,在实现均匀二维周期性结构的过程中,该技术对于实验仪器设备的精密度要求较高,入射角或者方位角的偏差都会使干涉图像出现调制现象。在应用四光束干涉时,根据强度调制空间分布需求,合理设置干涉光束的入射角和方位角,为实验制备中干涉参量的优化提供指导。

参 考 文 献

- [1] Liu Y, Liu S, Zhang X. Fabrication of three-dimensional photonic crystals with two-beam holographic lithography [J]. *Applied Optics*, 2006, 45(3): 480-483.
- [2] Lin Y, Harb A, Lozano K, *et al.* Five beam holographic lithography for simultaneous fabrication of three dimensional photonic crystal templates and line defects using phase tunable diffractive optical element[J]. *Optics Express*, 2009, 17(19): 16625-16631.
- [3] Burrow G M, Gaylord T K. Multi-beam interference advances and applications: nano-electronics, photonic crystals, metamaterials, subwavelength structures, optical trapping, and biomedical structures [J]. *Micromachines*, 2011, 2(2): 221-257.
- [4] Krishnamoorthy A, Chanda K, Murarka S P, *et al.* Self-assembled near-zero-thickness molecular layers as diffusion barriers for Cu metallization[J]. *Applied Physics Letters*, 2001, 78(17): 2467-2469.
- [5] Kruger J, Plass R, Cevey L, *et al.* High efficiency solid-state photovoltaic device due to inhibition of interface charge recombination [J]. *Applied Physics Letters*, 2001, 79(13): 2085-2087.
- [6] Xu D, Chen K P, Ohlinger K, *et al.* Nanoimprinting lithography of a two-layer phase mask for three-dimensional photonic structure holographic fabrications via single exposure[J]. *Nanotechnology*, 2011, 22(3): 035303.
- [7] Goldenberg L M, Lisinetskii V, Gritsai Y, *et al.* Second order DFB lasing using reusable grating inscribed in azobenzene-containing material [J]. *Optical Materials Express*, 2012, 2(1): 11-19.
- [8] Ebendorff-Heidepriem H, Ehrt D. Formation and UV absorption of cerium, europium and terbium ions in different valencies in glasses [J]. *Optical Materials*, 2000, 15(1): 7-25.
- [9] Goldenberg L M, Gritsai Y, Kulikovska O, *et al.* Three-dimensional planarized diffraction structures based on surface relief gratings in azobenzene materials[J]. *Optics Letters*, 2008, 33(12): 1309-1311.
- [10] Zhou X P, Shu J, Lu B J, *et al.* Two-wavelength division demultiplexer based on triangular lattice photonic crystal resonant cavity [J]. *Acta Optica Sinica*, 2013, 33(1): 0123001.
周兴平, 疏静, 卢斌杰, 等. 基于三角晶格光子晶体谐振腔的双通道解波分复用器[J]. *光学学报*, 2013, 33(1): 0123001.
- [11] Isakov D S, Kundikova N D, Miklyaev Y V. Interference lithography for the synthesis of three-dimensional lattices in SU-8: interrelation between porosity, an exposure dose and a grating period[J]. *Optical Materials*, 2015, 47: 473-477.
- [12] Xiong P X, Jia X, Jia T Q, *et al.* Two-dimensional complex nano-micro patterning on GaP and ZnSe surface created by the interference of three femtosecond laser beams [J]. *Acta Physica Sinica*, 2010, 59(1): 311-316.
熊平新, 贾鑫, 贾天卿, 等. 三光束飞秒激光干涉在 GaP, ZnSe 表面诱导二维复合纳米-微米周期结构 [J]. *物理学报*, 2010, 59(1): 311-316.
- [13] Yang H D, Li X H, Li G Q, *et al.* Silicon surface microstructures created by 1064 nm Nd : YAG nanosecond laser [J]. *Acta Physica Sinica*, 2011, 60(2): 027901.
杨宏道, 李晓红, 李国强, 等. 1064 nm 纳秒脉冲激光诱导硅表面微结构研究 [J]. *物理学报*, 2011, 60(2): 027901.
- [14] Li C, Cheng G H, Stoian R. Investigation of femtosecond lase-induced periodic surface structure ontungsten [J]. *Acta Optica Sinica*, 2016, 36(5): 0532001.
李晨, 程光华, Stoian R. 飞秒激光诱导金属钨表面周期性自组织结构的研究 [J]. *光学学报*, 2016, 36(5): 0532001.

- [15] Zhong M L, Li Y. Special introduction: ultra-fast laser processing and micro-nano manufacturing [J]. Chinese Journal of Laser, 2017, 44(1): 0102000. 钟敏霖, 李焱. “超快激光加工与微纳制造”专题前言 [J]. 中国激光, 2017, 44(1): 0102000.
- [16] Zhang J, Feng B R, Guo Y K. Theoretical analysis for fabricating nanometer hole array with 4 laser beams interferencelithography [J]. Acta Photonica Sinica, 2003, 32(4): 398-401. 张锦, 冯伯儒, 郭永康. 四激光束干涉光刻制造纳米级孔阵的理论分析 [J]. 光子学报, 2003, 32(4): 398-401.
- [17] Cheng X J, Zhang Z L, Ge H L. Fabricating three-dimensional periodic micro-structure with planar defects via a single exposure [J]. Acta Physica Sinica, 2012, 61(17): 174211. 陈小军, 张自丽, 葛辉良. 四光束干涉单次曝光构造含平面缺陷三维周期性微纳结构 [J]. 物理学报, 2012, 61(17): 174211.
- [18] Li Y, Chen H, Dai K J. Fabrication of graphene nanomeshes by the femtosecond four-beam interference technique [J]. Micronanoelectronic Technology, 2013, 50(10): 662-666. 李艳, 陈辉, 代克杰. 飞秒四光束干涉技术加工石墨烯纳米网 [J]. 微纳电子技术, 2013, 50(10): 662-666.
- [19] Zhang J, Feng B R, Guo Y K. Comparison between double exposure with two laser beams interference and single exposure with four laser beams [J]. Opto-Electronic Engineering, 2005, 32(12): 21-24. 张锦, 冯伯儒, 郭永康. 双光束双曝光与四光束单曝光干涉光刻方法的比较 [J]. 光电工程, 2005, 32(12): 21-24.
- [20] Liang W Y, He R B, Lin D R, *et al.* Influence of beam polarizations on holographic fabrication of triangular photonic crystals [J]. Laser & Optoelectronics Progress, 2016, 53(9): 091601. 梁文耀, 何锐斌, 林灯荣, 等. 光束偏振对三角光子晶体全息制作影响的仿真研究 [J]. 激光与光电子学进展, 2016, 53(9): 091601.
- [21] Wu X. Influence study of polarization on three-beam interference [J]. Acta Optica Sinica, 2015, 35(10): 1012002. 吴晓. 偏振态对三光束激光干涉分布的影响 [J]. 光学学报, 2015, 35(10): 1012002.
- [22] Wang D, Wang Z, Zhang Z, *et al.* Effects of polarization on four-beam laser interference lithography [J]. Applied Physics Letters, 2013, 102(8): 081903.
- [23] Zhang J, Wang Z, Di X, *et al.* Effects of azimuthal angles on laser interference lithography [J]. Applied Optics, 2014, 53(27): 6294-6301.
- [24] Ma L N, Zhang J, Jiang S L, *et al.* Influence of patterns quality of multi-beam interference lithography caused by the deviations of incidence azimuth angle and intensity of light [J]. Acta Photonica Sinica, 2015, 44(10): 1011003. 马丽娜, 张锦, 蒋世磊, 等. 入射光束角度及强度偏差对多光束干涉光刻结果的影响 [J]. 光子学报, 2015, 44(10): 1011003.